

Does the tracer gradient vector align with the strain eigenvectors in 2D turbulence?

G. Lapeyre,^{a)} P. Klein, and B. L. Hua

Laboratoire de Physique des Océans, IFREMER, BP 70, 29280 Plouzané, France

(Received 22 January 1999; accepted 20 August 1999)

This paper investigates the dynamics of tracer gradient for a two-dimensional flow. More precisely, the alignment of the tracer gradient vector with the eigenvectors of the strain-rate tensor is studied theoretically and numerically. We show that the basic mechanism of the gradient dynamics is the competition between the effects due to strain and an effective rotation due to both the vorticity and to the rotation of the principal axes of the strain-rate tensor. A nondimensional criterion is derived to partition the flow into different regimes: In the strain dominated regions, the tracer gradient vector aligns with a direction different from the strain axes and the gradient magnitude grows exponentially in time. In the strain-effective rotation compensated regions, the tracer gradient vector aligns with the bisector of the strain axes and its growth is only algebraic in time. In the effective rotation dominated regions, the tracer gradient vector is rotating but is often close to the bisector of the strain axes. A numerical simulation of 2D (two-dimensional) turbulence clearly confirms the theoretical preferential directions in strain and effective rotation dominated regions. Effective rotation can be dominated by the rotation rate of the strain axes, and moreover, proves to be larger than strain rate on the periphery of vortices. Taking into account this term allows us to improve significantly the Okubo–Weiss criterion. Our criterion gives the correct behavior of the growth of the tracer gradient norm for the case of axisymmetric vortices for which the Okubo–Weiss criterion fails. © 1999 American Institute of Physics. [S1070-6631(99)01312-4]

I. INTRODUCTION

The study of 2D turbulence is known to be pertinent to the understanding of large-scale geophysical flows of the extra-tropical atmosphere or ocean. These large-scale flows are characterized by coherent vortices where most of the enstrophy is concentrated. The process of filamentation creates very sharp gradients of vorticity at the edge of the vortices and produces small-scale filaments-like structures.¹ These filaments are stretched and folded by the velocity field between the large-scale vortices. This process is the manifestation of the enstrophy cascade which knowledge in physical space is important to better understand the internal organization of the flow.

Within this context, the approach followed by many studies^{2–5} has been to examine the dynamics of vorticity gradient, or more generally, of the gradient of a tracer which is conserved along a Lagrangian trajectory; such tracer gradient obeys the same equation as vorticity gradient. The gradients dynamics allow to partition the physical space into different regions: Production regions where tracer gradient norm grows exponentially and regions where the evolution of gradient norm is slow and where gradient rotation is expected.

Okubo² and Weiss³ were the first to derive a criterion based on the eigenvalues of the velocity gradient tensor which governs the equation of the first order time derivative of the tracer gradient vector. They assumed that the velocity gradient tensor is slowly varying along a Lagrangian trajec-

tory. However counter-examples, such as the point-vortex flow, show that a criterion involving only these eigenvalues is not sufficient. Subsequent studies^{4,6} have shown that the acceleration gradient tensor (or the pressure Hessian), which governs the second-order time derivative of the tracer gradient vector is also an important quantity to consider, thus invalidating the assumptions of Okubo and Weiss.

An alternative approach in the study of the enstrophy cascade, noted by McWilliams,⁷ is to examine the exponential growth rate of the vorticity gradient norm. This growth rate depends on two quantities: The positive eigenvalue of the rate-of-strain tensor and the angle between its compressional eigenvector and the vorticity gradient. The knowledge of the eigenvalue cannot solely determine the growth rate. The determination of the orientation of the vorticity gradient with respect to the compressional eigenvector is essential in order to understand the enstrophy cascade.

A remark of Babiano *et al.*⁸ indicates the possible existence of some alignment properties in 2D flows: They noted that isolines of tracer and vorticity have similar orientations. These two tracers are likely to align with the same direction which depends only on the flow topology. Other studies^{5,9,10} have revealed a tendency for vorticity gradient to align with the compressional eigenvector. The issue of alignment with the eigenvector of the strain-rate tensor has also been extensively studied in 3D (three-dimensional) turbulence. It has been shown numerically^{11–14} that the tracer gradient (or the vorticity vector¹⁵) tends to align with an eigenvector of the rate-of-strain tensor. With an assumption similar to that made by Okubo and Weiss, this result for the vorticity vector

^{a)}Electronic mail: glapeyre@ifremer.fr

can be demonstrated,¹⁶ thus stressing the importance of the invariants of the velocity gradient tensor. In 2D turbulence, a single invariant remains: The determinant of the tensor, which is the opposite of the Okubo–Weiss quantity. Recent 3D results have revealed that the assumption is not always valid and that the pressure Hessian plays an important role.^{17,18} These results show many similarities between 2D and 3D turbulence.

This paper revisits the question of the alignment of vorticity or tracer gradient with the eigenvectors of the rate-of-strain tensor, and more generally, the existence of a preferential direction for the gradient vector. In Sec. II, the equation for the orientation of tracer gradient in the strain basis is derived, following the approach of Dresselhaus and Tabor¹⁹ (which was also used by Dritschel *et al.*²⁰ to examine the stability of vorticity filaments). This basis allows to take into account explicitly the part of the acceleration gradient tensor that corresponds to the rotation of the strain axes. In Sec. III, the orientation equation is solved assuming a stationarity property for the velocity field which is much less restrictive than the Okubo–Weiss assumption. We propose a new criterion to partition the physical space into strain dominated regions and effective rotation dominated regions, where effective rotation is defined as the sum of the vorticity and the rotation rate of the strain axes. Furthermore, we provide an estimation for both the direction of the gradient vector and the exponential growth rate of its norm. These results allow to characterize the tracer cascade in physical space. In Sec. IV, the accuracy of our results is assessed through the examination of a numerical simulation of freely decaying turbulence and through analytical examples. It is shown that our criterion yields an exact solution of the growth rate of gradient norm for axisymmetric vortices (which the point-vortex belongs to) and an improved approximation of the growth rates in 2D turbulence.

II. EQUATIONS FOR THE EVOLUTION OF TRACER GRADIENT

A. Magnitude and orientation

Let us consider a tracer q which is conserved along a Lagrangian trajectory in a two-dimensional flow field

$$\frac{Dq}{Dt} \equiv \partial_t q + \mathbf{u} \cdot \nabla q = 0, \quad (1)$$

where $\mathbf{u} = (u, v)$ and $\nabla \cdot \mathbf{u} = 0$.

In a more general situation, there should be a diffusive term ($\nu \nabla^2 q$) on the right hand side of Eq. (1). Its main effect is to weaken the gradient magnitude. We assume in this study that the dynamics of tracer gradient orientation is insensitive to this diffusive term.

The equation for the tracer gradient is

$$\frac{D\nabla q}{Dt} = -[\nabla \mathbf{u}]^* \nabla q, \quad (2)$$

where $[\nabla \mathbf{u}]^*$ is the transpose of the velocity gradient tensor.

For what follows, some definitions have to be given:

$$\begin{aligned} \sigma_n &= \partial_x u - \partial_y v, & \nabla q &= \rho(\cos \theta, \sin \theta), \\ \sigma_s &= \partial_x v + \partial_y u, & (\sigma_s, \sigma_n) &= \sigma(\cos 2\phi, \sin 2\phi), \\ \omega &= \partial_x v - \partial_y u, & \text{with } \rho &\geq 0 \text{ and } \sigma \geq 0. \end{aligned}$$

The eigenvectors of the rate-of-strain matrix (the symmetric part of $[\nabla \mathbf{u}]^*$) are called the compressional and extensional strain axes. The compressional axis corresponds to the maximum growth rate of gradient norm, whereas the extensional axis corresponds to the maximum decay rate. The angle between the x axis and the compressional axis is $-\pi/4 - \phi$.

As Eq. (2) is dependent on the coordinates system, it is more convenient to separate the magnitude of the tracer gradient from its orientation

$$\frac{1}{\rho^2} \frac{D\rho^2}{Dt} = -\sigma \sin(2(\theta + \phi)), \quad (3)$$

$$2 \frac{D\theta}{Dt} = \omega - \sigma \cos(2(\theta + \phi)). \quad (4)$$

The right-hand-side of Eq. (3) indicates that the evolution of the magnitude ρ strongly depends on the angle between the tracer gradient and the eigenvectors of the rate-of-strain matrix. This emphasizes the importance of the orientation dynamics. By contrast, Eq. (4) for the orientation θ does not depend on the gradient magnitude ρ .

The same equations have also been derived by Dresselhaus and Tabor¹⁹ and Dritschel *et al.*²⁰ Dritschel *et al.*²⁰ investigate the stability of a vorticity filament submitted to strain. They show that if the stretching rate γ exceeds 25% of the vorticity anomaly $\delta\omega$ (the typical vorticity contrast across the filament), the instability is completely suppressed. Another possibility to inhibit roll-up instability is the presence of adverse shear $\Lambda/\delta\omega < 0$ where Λ is the twisting rate. In our notations, these quantities are simply:

$$\gamma \equiv \frac{1}{\rho} \frac{D\rho}{Dt} = -\frac{\sigma}{2} \sin(2(\theta + \phi))$$

$$\Lambda = 2 \frac{D\theta}{Dt} - \omega = -\sigma \cos(2(\theta + \phi)).$$

Dritschel²¹ uses these diagnostics in a simulation of 2D turbulence where he shows that most of the vorticity filaments behave passively. A prediction of the orientation of the vorticity gradient would lead to a better identification of the regions where vorticity filaments should remain passive. The important role played by the rotation of the strain-rate axes relatively to vorticity, was not stressed by Dritschel *et al.*^{20,21} In contrast, in the present paper, we provide evidence that it allows to better characterize the stirring properties in physical space.

B. Orientation in strain coordinates

In order to simplify Eq. (4), we define

$$\zeta = 2(\theta + \phi) \quad \text{and} \quad \tau = \int_0^t \sigma(s) ds. \quad (5)$$

We expect the orientation ζ to be a continuous function of time, so its values are to be taken in $[-\infty, \infty]$ and not in

[0,2π]. It is related to the angle between the tracer gradient and the strain axes: A value of π/2 (respectively, -π/2) stands for an alignment with the compressional (resp. extensional) axis. τ is related to the strain-rate history experienced by a fluid particle (t is here the Lagrangian time). The typical time for the process of alignment is thus given by the inverse of the rate-of-strain and is much shorter than the time taken for the diffusion to act if it were present. Equation (4) becomes a simple first-order O.D.E. (ordinary differential equation)

$$\frac{D\zeta}{D\tau} = r - \cos \zeta, \tag{6}$$

with

$$r = \frac{\omega}{\sigma} + 2 \frac{D\phi}{D\tau} = \frac{\omega + 2(D\phi/Dt)}{\sigma}.$$

The dimensionless parameter r is the ratio between effective rotation (in the terminology of Dresselhaus and Tabor¹⁹) in the strain basis (i.e., the rotation effects due to both the vorticity and the rotation of the principal axes of the strain-rate tensor) and the magnitude of the strain rate (which tends to align the gradient with a strain eigenvector).

The Lagrangian time derivative of φ is simply related to the Lagrangian time derivatives of σ_n and σ_s

$$2 \frac{D\phi}{Dt} = \frac{\sigma_s(D\sigma_n/Dt) - \sigma_n(D\sigma_s/Dt)}{\sigma_n^2 + \sigma_s^2}.$$

These quantities can be expressed as functions of the Lagrangian acceleration gradient tensor. In two dimensions, the Lagrangian acceleration is equal to the pressure gradient, and the quantities to examine are given by

$$\frac{D\sigma_n}{Dt} = -(\partial_{xx} - \partial_{yy})p, \tag{7a}$$

$$\frac{D\sigma_s}{Dt} = -2\partial_{xy}p, \tag{7b}$$

where p is the pressure.

Basdevant and Philipovitch⁶ and Hua and Klein⁴ have shown that (1/σ)(Dσ/Dt) and Dφ/Dt are of the same order of magnitude as σ and ω (involved in the Okubo–Weiss criterion). Thus their effects need to be included to obtain the exact gradient dynamics. Here our main assumptions are that (i) the parameter r and (ii) the rate of strain σ are slowly varying along a Lagrangian trajectory. This allows to solve Eq. (6) and to recover t from τ. Thus we focus our attention on the competition between strain and effective rotation by taking into account the role of the rotation of the strain axes (Dφ/Dt) but we neglect (1/σ)(Dσ/Dt).

III. DYNAMICS OF THE GRADIENT ORIENTATION

A. Different regimes of evolution

A first examination of Eq. (6) (Fig. 1) shows that

- if r²<1, there are two fixed points, one stable ζ₋ and one unstable ζ₊. Moreover ζ should converge to the stable fixed point ζ₋,

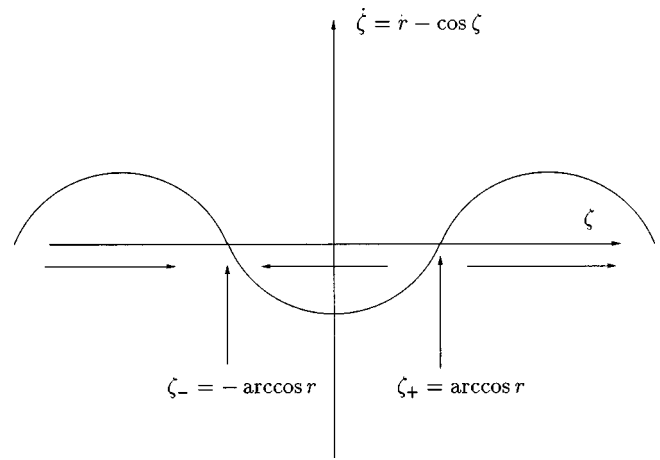


FIG. 1. Diagram of the behavior of ζ for r²<1.

- if r²>1, Dζ/Dτ = r - cos ζ ~ r and ζ should grow quasi-linearly in time.

We recognize a partition of the flow similar to the partition of Okubo² and Weiss³ into hyperbolic (or “straining”) regions (r²<1) and elliptic (or “eddy”) regions (r²>1). The main difference is that we take into account the rotation of the strain axes.

The general solutions of Eqs. (3) and (6) for the three regimes r²<1, r²=1 and r²>1 are now presented.

1. Strain dominated regions: r²<1

The general solution is

$$\zeta(\tau) = -2 \arctan \left(\sqrt{\frac{1-r}{1+r}} \tanh \left(A + \frac{\tau \sqrt{1-r^2}}{2} \right) \right), \tag{8}$$

$$\rho^2(\tau) = \rho_0^2 \frac{r + \cosh(2A + \tau \sqrt{1-r^2})}{r + \cosh(2A)}. \tag{9}$$

Here the constant A is the same for the two equations and depends on the initial orientation of the tracer gradient.

The gradient orientation converges to the direction²²

$$\zeta_- = -\arccos r, \tag{10}$$

exponentially fast. This preferential direction corresponds to a stable fixed point and does not depend on the initial direction of the gradient vector. This direction is different from the strain eigenvectors except for r=0. However, the two fixed directions are related to the eigenvectors of the velocity gradient tensor seen in the strain basis as proven in Appendix. This alignment is associated with an exponential gradient growth with a dimensional rate $\sqrt{\sigma^2 - (\omega + 2(D\phi/Dt))^2}$. This regime should correspond to regions where particles are expelled very rapidly, for instance in the saddle points of the flow.

2. Strain-effective rotation compensated regions: r²=1

The general solution is

$$\zeta(\tau) = \frac{\pi}{2} (1+r) + 2 \arctan(A + r\tau), \tag{11}$$

$$\rho^2(\tau) = \rho_0^2 \frac{1 + (A + r\tau)^2}{1 + A^2}. \tag{12}$$

The gradient orientation converges to the direction

$$\zeta_- = \frac{1 - r}{2} \pi, \tag{13}$$

which makes an angle of $\pi/4$ with the strain axes. The convergence is slower than for the preceding regime. It is associated with an algebraic growth of the gradient magnitude. This process of slow growth could maintain sharp gradients of tracer as in the case of axisymmetric vortices and shear flows (these cases are studied in Sec. IV B).

3. Effective rotation dominated regions: $r^2 > 1$

The general solution is

$$\zeta(\tau) = 2 \arctan \left(\sqrt{\frac{r-1}{r+1}} \tan \left(A + \text{sign}(r) \frac{\sqrt{r^2-1}}{2} \tau \right) \right), \tag{14}$$

$$\rho^2(\tau) = \rho_0^2 \frac{r + \cos(2A + \text{sign}(r) \tau \sqrt{r^2-1})}{r + \cos(2A)}. \tag{15}$$

Actually Eq. (14) is quasi linear in time (remember that ζ is a continuous function of time): $\zeta \sim \text{sign}(r) \tau \sqrt{r^2-1}$. This means that the gradient vector is rotating in the strain basis because of either the rotation of the strain axes or the effect of vorticity. In the coordinates (x, y) , the dimensional rotation rate is: $(\omega + 2(D\phi/Dt))\sqrt{1-r^{-2}} - 2(D\phi/Dt)$. Thus, for large values of r , the gradient rotates at the angular velocity ω .

However, there is a preferential direction

$$\zeta_{\text{prob}} = \frac{1 - \text{sign}(r)}{2} \pi. \tag{16}$$

The reason for the existence of this direction is that when $\zeta = \zeta_{\text{prob}}$, $|(D\zeta/D\tau)|$ is minimum. So the tracer gradient spends more time near this direction than near other directions and, on time average, the gradient direction will lie near ζ_{prob} . Moreover, according to Eq. (15), the gradient magnitude remains bounded. This situation should correspond to the cores of vortices or regions of rapid strain axes rotation.

B. Criterion to partition the flow

According to the preceding results, the criterion r allows to partition the fluid in three regimes with different properties concerning the tracer gradient evolution:

1. if $r^2 < 1$, the effects of strain dominate. The gradient orientation ζ converges to the direction $\zeta_- = -\arccos r$; the gradient magnitude grows exponentially in time at the non-dimensional rate $\sqrt{1-r^2}$.
2. if $r^2 = 1$, the effects of strain and effective rotation balance each other. The direction tends to $\zeta_- = (1-r)\pi/2$ which is the bisector of the strain axes. The magnitude of the gradient grows only algebraically in time.
3. if $r^2 > 1$, effective rotation dominates. The direction rotates in the reference frame of the strain axes because of

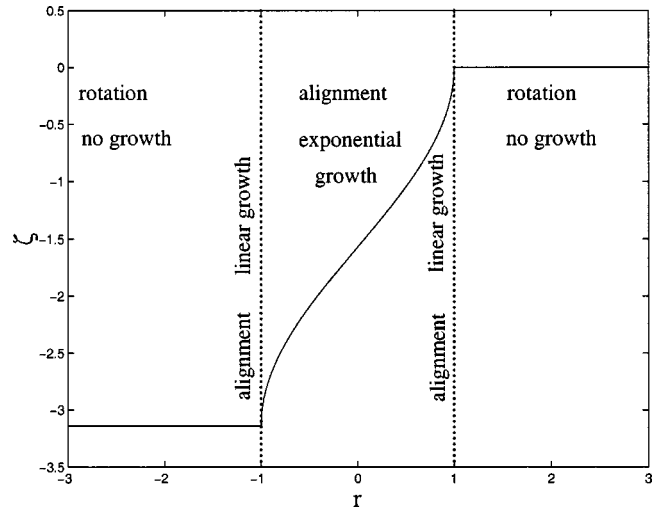


FIG. 2. Preferential direction ζ and nature of the dynamics of gradient as a function of r .

the rotation due to vorticity and of the rotation of the strain axes. However the most probable direction is $\zeta_{\text{prob}} = [1 - \text{sign}(r)] \pi/2$ which makes an angle of $\pi/4$ with the strain axes. The nondimensional rotation rate is $\sqrt{r^2-1}$ in the strain coordinates. The magnitude of the gradient does not grow nor decay.

Figure 2 summarizes the different regimes of the gradient dynamics and the preferential directions as a function of r . An approach based on the eigenvalues of the velocity gradient tensor expressed in the strain basis gives the same results (see Appendix).

IV. NUMERICAL AND ANALYTICAL RESULTS

A. Freely decaying turbulence

We diagnose a numerical simulation of freely decaying turbulence at a resolution of 1024×1024 using a pseudo-spectral code (see Hua and Klein⁴ for more details). There is a Newtonian viscosity such that the Reynolds number is 3.5×10^4 . It should not affect the gradient orientation dynamics as the following results seem to indicate. The flow exhibits the emergence of coherent structures together with a strong filamentation in the vorticity field (Fig. 3).

The probability density function for r (Fig. 4, curve A) presents a slight asymmetry between positive and negative values of r with a plateau between -1 and 1 . Strong vorticity gradients (which represent 2% in area as indicated in the figure caption) seem to prefer regions where $r^2 = 1$ (curve B), a result which stresses the dominance of this regime. The fraction of hyperbolic regions (defined as $r^2 < 1$) represents 59% of the total field. The asymmetry between the area of elliptic and hyperbolic regions was also noted by Protas *et al.*⁵ but based on the Okubo–Weiss definition (i.e., without the rotation of the strain axes).

The key result of this study is displayed on Figs. 5(a) and 5(b) which compare the alignments of the vorticity gradient vector with the compressional strain axis and with the direction given by the preferential directions ζ_- [Eq. (10)] and ζ_{prob} [Eq. (16)]. We concentrate on regions with strong

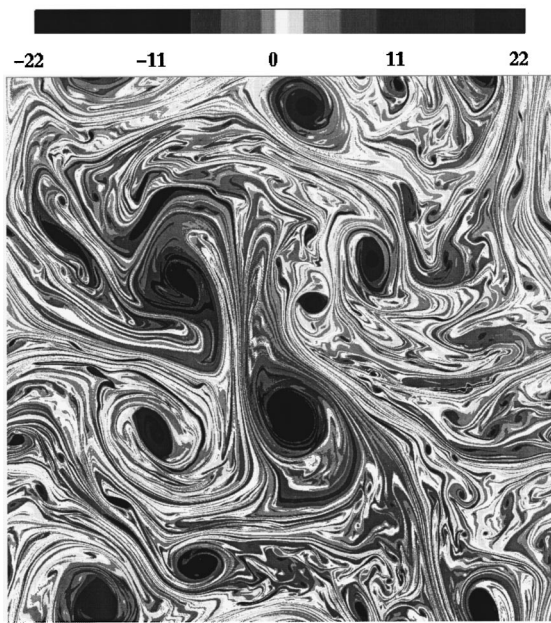


FIG. 3. Vorticity ω . Dark regions represent vorticity extrema.

gradients because pdfs are sharper there but the results also hold for the entire field (not shown). The alignment with the compressional axis in the regime $r^2 \leq 1$ is represented by curve A on Fig. 5(a). A value of 0 (respectively, $\pm \pi$) corresponds to the case where the vorticity gradient is aligned with the compressional (resp. extensional) axis. There is a weak tendency for alignment with the compressional axis. However experimental results reveal a much better alignment of the vorticity gradients with the direction corresponding to the stable solution ζ_- of Eq. (10) (curve B). In the

regime $r^2 > 1$ [Fig. 5(b)], the gradient orientation (curve A) exhibits a weak preference for no exponential growth ($\sin \zeta \sim 0$). On contrast, curve B shows that gradients are close to the most probable direction ζ_{prob} [Eq. (16)]. The comparison of the curves B of Figs. 5(a) and 5(b) reveals a narrow peak for $r^2 \leq 1$ and a broader one for $r^2 > 1$. This could point out the existence of a mechanism of alignment in regime $r^2 \leq 1$ and the absence of such a mechanism in regime $r^2 > 1$. Figures 5(a) and 5(b) confirm that our analytical solution reproduces rather well the basic features of vorticity gradient dynamics.

Figure 6 presents the joint p.d.f. of $\zeta + \pi/2$ and r , the bold curve is $\cos \zeta$. The relation $\cos \zeta \sim r$ is well corroborated and this strongly validates the analytical solution. A joint p.d.f. between ζ and ω/σ (not shown) does not present such a correlation, thus further emphasizing the quantitative importance of the rotation of the strain axes.

For $r^2 < 1$, the area of regions of gradient norm decay represents only 36% of the total area. These regions are generally associated with the alignment with the unstable direction $\zeta_+ = +\arccos r$ (not shown). This alignment is not as strong as with ζ_- in regions of growth.

Now we can examine the distributions of vorticity ω , the parameter r and the exponential gradient growth rate $-\sigma \sin \zeta$ in physical space [Figs. 7(a)–7(c)] to understand their importance. We focus our attention on a single vortex as all vortices display a similar behavior. Figure 7(a) presents the vorticity contours of the anticyclonic vortex close to the center of Fig. 3. The core of the vortex is surrounded by filaments peeled out as described by Mariotti *et al.*¹ Some are expelled far away from the vortex.

Figure 7(b) represents the field of r . At first glance, we

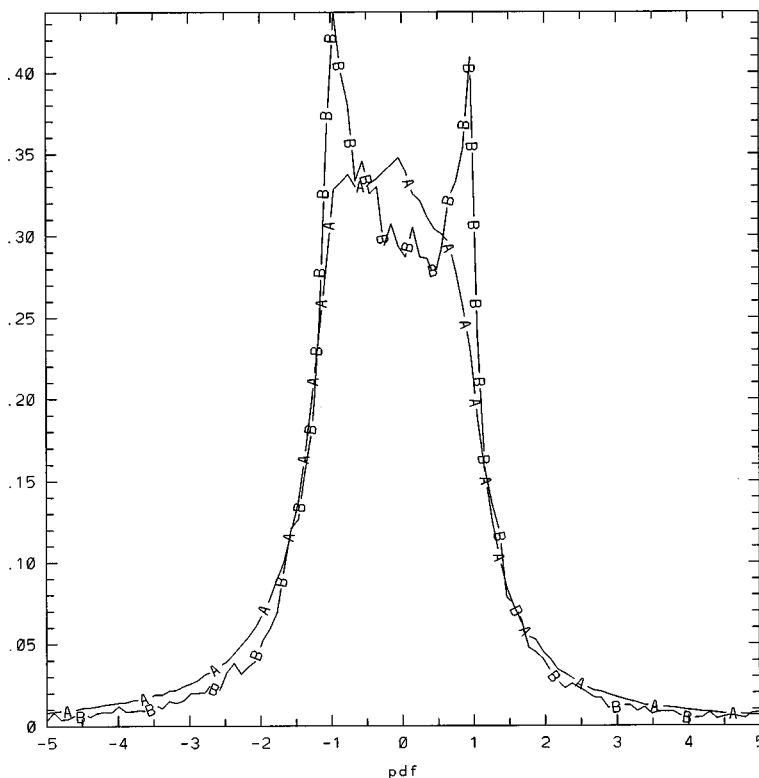


FIG. 4. p.d.f. of r , A: Total field, B: For $|\nabla q| > 600$ (2%).

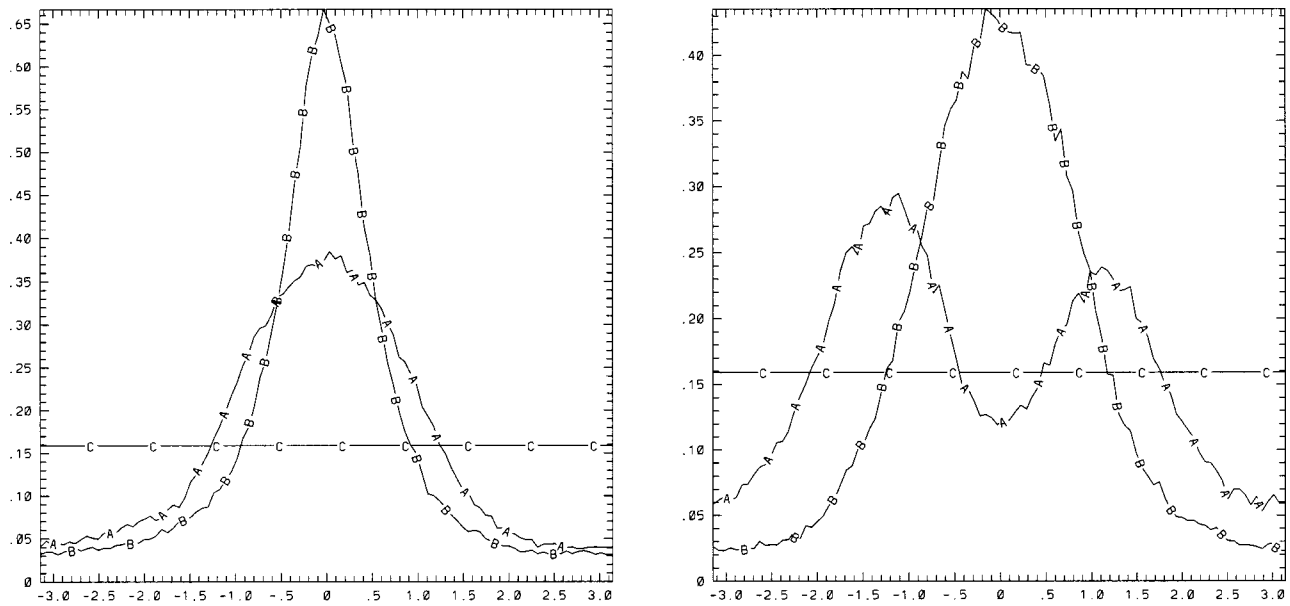


FIG. 5. (a) Alignment p.d.f. for $|\nabla q| > 200$ and $r^2 \leq 1$ (17%), A: Of $\zeta + \pi/2$, B: Of $\zeta - \zeta_{\text{prob}}$, C: Equi-partitioned p.d.f. (b) alignment for $|\nabla q| > 200$ and $r^2 > 1$ (10%), A: p.d.f. of $\zeta + \pi/2$, B: p.d.f. of $\zeta - \zeta_{\text{prob}}$, C: Equi-partitioned p.d.f.

see that r is a good index for the characterization of the topology of vortices since the different dynamical regimes (corresponding to different values of r) are well separated in physical space. The vortex core is a region with $r < -1$ because of large ω . The vortex periphery is composed of regions with $r^2 < 1$ because of large σ and regions with $r > 1$ because of large $(D\phi/Dt)$. For each vortex, we observe opposite signs of r between its core and the part on its periphery where effective rotation is strong. In these regions, $\omega + 2(D\phi/Dt)$, is dominated by $2(D\phi/Dt)$ which is of oppo-

site sign of ω . This indicates that a characterization of the stirring properties of vortices must take into account this rotation rate.

A comparison with the exponential gradient growth rate $-\sigma \sin \zeta$ [Fig. 7(c)] reveals that the regions of maximum exponential growth or decay rate are characterized by $r^2 < 1$. Regions of gradient norm growth are contiguous to regions of decay, and these two types of regions are well separated by sharp fronts. The small growth rates on the vortex edge are associated with strong values of the parameter r .

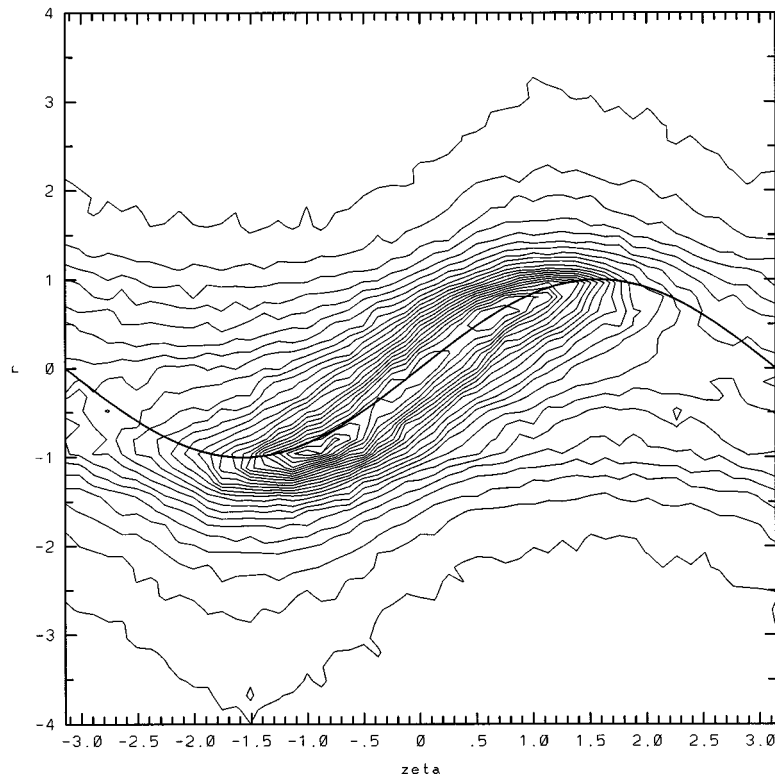


FIG. 6. Joint p.d.f. of $\zeta + \pi/2$ and r (total field); the bold curve is $\cos \zeta$.

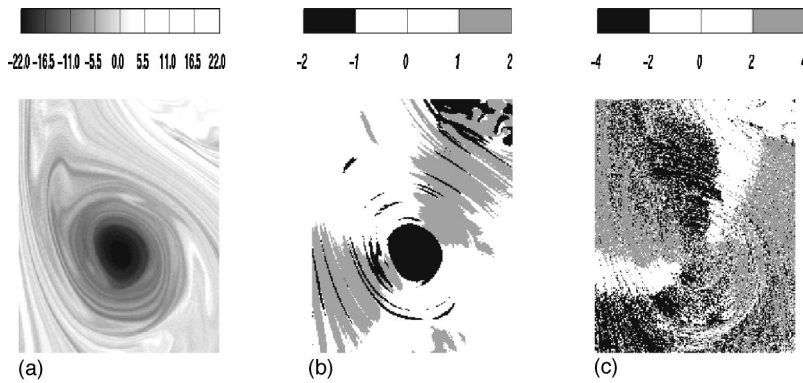


FIG. 7. (a) Vorticity ω . (b) Criterion, $r = (\omega + 2(D\phi/Dt))/\sigma$. (c) Exponential gradient growth rate $-\sigma \sin \zeta$.

Finally, the core of the vortex presents strong growth of gradient, and other mechanisms like diffusion may play a role there.

B. Analytic examples

To stress the physical importance of the regime $r^2 = 1$, we examine two analytical examples which are solutions of the Euler equations.

1. Axisymmetric vortices

Consider an axisymmetric vortex, that is a flow with a streamfunction $\psi(R)$ where $R^2 = x^2 + y^2$. Particles are rotating at the angular velocity $\Omega = -(1/R)(d\psi/dR)$. The rate of strain is $\sigma = |(1/R)(d\psi/dR) - (d^2\psi/dR^2)|$ while the vorticity is $\omega = (1/R)(d\psi/dR) + (d^2\psi/dR^2)$. Analytical solutions for tracer gradient are

$$\rho = \rho_0 \sqrt{\frac{1 + (A + r\sigma t)^2}{1 + A^2}}, \tag{17}$$

$$\zeta = \frac{\pi}{2} (1 + r) + 2 \arctan(A + r\sigma t), \tag{18}$$

with

$$r = \text{sign} \left(\frac{d^2\psi}{dR^2} - \frac{1}{R} \frac{d\psi}{dR} \right) = \pm 1. \tag{19}$$

The orientation ζ tends to $(1 - r)\pi/2$ so gradients become more and more radial: They rotate in physical space to follow the rotation of the strain axes. Moreover their magnitude is linearly increasing with time.

The Okubo–Weiss criterion is $\lambda_0 = \sigma^2 - \omega^2 = -2[(1/R)(d\psi/dR)(d^2\psi/dR^2)]$. Thus the criterion is either positive which indicates hyperbolic regions, or negative which indicates elliptic regions, according to the definitions given by Weiss. But the flow is neither elliptic nor hyperbolic since the gradient growth is only linear in time; this behavior occurs because of the rotation of the strain axis: $(D\phi/Dt) = -(1/R)(d\psi/dR)$, which is not taken into account by the Okubo–Weiss criterion and this criterion is therefore incorrect. On the contrary, the value of our criterion ($r = \pm 1$) predicts the alignment dynamics and the linear growth of tracer gradients.

2. Shear flows

Consider a shear flow such that $(u, v) = (u(y), 0)$. The rate of strain is $\sigma = |du/dy|$ and the vorticity $\omega = -(du/dy)$. This flow is similar to the previous one because the behavior of tracer gradient is

$$\rho = \rho_0 \sqrt{\frac{1 + (A + r\sigma t)^2}{1 + A^2}}, \tag{20}$$

$$\zeta = \frac{\pi}{2} (1 + r) + 2 \arctan(A + r\sigma t), \tag{21}$$

where

$$r = \text{sign} \left(-\frac{du}{dy} \right) = \pm 1. \tag{22}$$

The gradients tend to be oriented perpendicularly to the flow. Here the strain axes are fixed: $(D\phi/Dt) = 0$. So both the Okubo–Weiss criterion ($\lambda_0 = 0$) and our criterion ($r^2 = 1$) indicate a linear growth of gradient norm: The main difference between these criteria is that r provides an estimation of the orientation of the gradient vector and the growth rate of its amplitude.

V. CONCLUSION

We can answer the question asked in the title of this paper: Both the analytical and numerical results of this study show that the tracer gradient vector does not preferentially align with strain eigenvectors. There exists a preferential direction depending only on the flow topology which has been estimated analytically.

The analytical solutions have revealed that the main mechanism of the tracer gradient dynamics is a response to the competition between strain and effective rotation (i.e., the rotation effects due to both the vorticity and the rotation of the principal axes of the strain-rate tensor). This competition leads to preferential directions that are different from the strain axes. We have derived a criterion based on the parameter r to describe the flow topology in terms of tracer gradient evolution. This parameter measures the competition between strain and effective rotation. When strain dominates or is equal to effective rotation ($r^2 \leq 1$), the tracer gradient aligns with an eigenvector of the velocity gradient tensor expressed in the strain basis. The gradient norm growth is

exponential when strain dominates ($r^2 < 1$), and linear when there is compensation $r^2 = 1$. When effective rotation dominates ($r^2 > 1$), the gradient vector only rotates, but with a tendency to align with the direction ζ_{prob} .

The numerical simulation clearly confirms that the competition mechanism is the main feature of alignment dynamics. The gradients are statistically well aligned with the estimated preferential directions. The criterion r allows to partition the flow into regions of exponential growth and regions of slow or no growth. Moreover the different patterns of the flow are well diagnosed by this criterion.

The preferential directions found in each regime allow us to estimate roughly the true stretching rate (i.e., the exponential growth rate), and thus to better precise the topology of the stirring. Moreover these results have revealed that the alignment properties of the tracer gradient vector do not depend on either the gradient magnitude or the orientation history. This explains why different tracer fields display strong gradients at the same locations and why their isolines are quite similar, as previously noted by Babiano *et al.*⁸ in their experiments.

Another important factor in tracer gradient dynamics is the rotation of the strain axes. Taking into account this term in the effective rotation effects allows a much better characterization of the stirring properties. An illustration of this point is that our criterion gives the correct behavior for tracer gradient for axisymmetric flows for which the Okubo–Weiss criterion is known to fail. The numerical simulation have also revealed that the rotation rate of the strain axes can be the predominant term of the effective rotation on the periphery of vortices. The reason is that the rotation of the strain axis is a part of the acceleration gradient tensor. The crucial role played by the Lagrangian accelerations for the stirring properties has been stressed by the work of Hua and Klein⁴ and Hua *et al.*²³ Even though we neglect the other part of the acceleration gradient tensor (that involves the Lagrangian time derivative of the strain rate), we obtain robust results since they have been confirmed by the numerical simulation and the analytical examples. It should be interesting to assess the effect of this other part, which requires a different approach. Such work is under progress.²⁴

The Lagrangian accelerations also play a key role for the stirring properties of more realistic flows as the quasi-geostrophic (QG) ones.²³ In such QG flows, not only the ageostrophic pressure [as in the 2D flows of the present study, see Eq. (7)] but also additional terms such as the beta effect and the divergence potential are present in the Lagrangian accelerations.²³ So future work should aim to extend the results of the present study to more realistic flows by considering the effects of these additional terms.

Finally, the role of diffusion on the alignment properties needs to be examined. Preliminary results indicate that its effect on alignment properties appears to be weak. This is also confirmed in this paper by the comparison of the inviscid analytical results with a numerical simulation that involves a Newtonian viscosity.

APPENDIX: EIGENVALUE PROBLEM

It is interesting to associate the O.D.E. approach of this paper with the eigenvalue approach of Okubo,² Weiss,³ and Hua and Klein⁴ because this latter approach can give the same kind of information. We start from the equation

$$\frac{D\nabla q}{Dt} = -[\nabla \mathbf{u}]^* \nabla q. \quad (\text{A1})$$

A change of basis allows to study more carefully this problem. The transform of orthonormal basis corresponds to a rotation of the gradient

$$\nabla q = R(\varphi) \mathbf{Y}. \quad (\text{A2})$$

Here $R(\varphi)$ is the rotation matrix of angle φ which will be defined later

$$R(\varphi) = \begin{pmatrix} \cos \varphi & -\sin \varphi \\ \sin \varphi & \cos \varphi \end{pmatrix}. \quad (\text{A3})$$

Now we decompose $[\nabla \mathbf{u}]^*$ in symmetric and antisymmetric parts

$$[\nabla \mathbf{u}] = S + \frac{\omega}{2} R\left(\frac{\pi}{2}\right), \quad (\text{A4})$$

where $[S]$ is the rate-of-strain matrix. The problem reduces into

$$\frac{D\mathbf{Y}}{Dt} = -\left(R(-\varphi)SR(\varphi) + \left(\frac{D\varphi}{Dt} - \frac{\omega}{2}\right)R\left(\frac{\pi}{2}\right)\right)\mathbf{Y}. \quad (\text{A5})$$

We can diagonalize $[S]$ with the appropriate φ ; it suffices to write it as

$$S = \frac{\sigma}{2} \begin{pmatrix} \sin 2\phi & \cos 2\phi \\ \cos 2\phi & -\sin 2\phi \end{pmatrix}. \quad (\text{A6})$$

Taking $\varphi = \pi/4 - \phi$, the tracer gradient in strain basis verifies

$$\frac{D\mathbf{Y}}{Dt} = \frac{\sigma}{2} \begin{pmatrix} -1 & -r \\ r & 1 \end{pmatrix} \mathbf{Y}. \quad (\text{A7})$$

The eigenvalues and eigenvectors of the matrix present in this equation are

$\mathbf{e}_1 = (-\cos \vartheta, \sin \vartheta)$ associated with

$$\lambda_1 = -\frac{\sigma}{2} \sqrt{1-r^2}, \quad (\text{A8})$$

$\mathbf{e}_2 = (-\sin \vartheta, \cos \vartheta)$ associated with

$$\lambda_2 = \frac{\sigma}{2} \sqrt{1-r^2}. \quad (\text{A9})$$

Here $\vartheta = \pi/4 - (\arccos r)/2$. If r^2 is greater than 1, the eigenvalues are purely imaginary.

For $r^2 < 1$, it is straightforward to see that \mathbf{e}_1 corresponds to $\zeta = \arccos r = \zeta_+$ and \mathbf{e}_2 to $\zeta = -\arccos r = \zeta_-$. So the eigenvectors and the eigenvalues of the velocity gradient tensor in the strain basis give the same information as our results. However, they are only a mean to know the dynamics of tracer gradients: They do not explain why this is the correct behavior. The approach of solving the O.D.E. enables to

shed more light on the tracer gradient dynamics while the eigenvalue problem is useful to identify the role of the time evolving quantities as σ or r .

- ¹A. Mariotti, B. Legras, and D. G. Dritschel, "Vortex stripping and the erosion of coherent structures in two-dimensional flows," *Phys. Fluids A* **6**, 3954 (1994).
- ²A. Okubo, "Horizontal dispersion of floatable particles in the vicinity of velocity singularity such as convergences," *Deep-Sea Res.* **17**, 445 (1970).
- ³J. Weiss, "The dynamics of enstrophy transfer in two-dimensional hydrodynamics," *Physica D* **48**, 273 (1991).
- ⁴B. L. Hua and P. Klein, "An exact criterion for the stirring properties of nearly two-dimensional turbulence," *Physica D* **113**, 98 (1998).
- ⁵B. Protas, A. Babiano, and N. K.-R. Kevlahan, "On geometrical alignment properties of two-dimensional forced turbulence," *Physica D* **128**, 169 (1999).
- ⁶C. Basdevant and T. Philipovitch, "On the validity of the 'Weiss criterion' in two-dimensional turbulence," *Physica D* **73**, 17 (1994).
- ⁷J. C. McWilliams, "The emergence of isolated coherent vortices in turbulent flow," *J. Fluid Mech.* **146**, 21 (1984).
- ⁸A. Babiano, C. Basdevant, B. Legras, and R. Sadourny, "Vorticity and passive-scalar dynamics in two-dimensional turbulence," *J. Fluid Mech.* **183**, 379 (1987).
- ⁹C. H. Gibson, W. T. Ashurst, and A. R. Kerstein, "Mixing of strongly diffusive passive scalars like temperature by turbulence," *J. Fluid Mech.* **194**, 261 (1988).
- ¹⁰K. Ohkitani and S. Kishiba, "Nonlocal nature of vortex stretching in an inviscid fluid," *Phys. Fluids A* **7**, 411 (1995).
- ¹¹W. Ashurst, W. Kerstein, and C. Gibson, "Alignment of vorticity and scalar gradient with strain rate in simulated Navier-Stokes turbulence," *Phys. Fluids* **30**, 2343 (1987).
- ¹²Z. S. She, E. Jackson, and S. Orszag, "Intermittent vortex structures in homogeneous isotropic turbulence," *Nature (London)* **344**, 226 (1990).
- ¹³G. R. Ruetich and M. R. Maxey, "Small scale features of vorticity and passive scalar fields in homogeneous isotropic turbulence," *Phys. Fluids A* **3**, 1587 (1991).
- ¹⁴A. Vincent and M. Meneguzzi, "The spatial and statistical properties of homogeneous turbulence," *J. Fluid Mech.* **225**, 1 (1991).
- ¹⁵The vorticity vector verifies the same equations as $\mathbf{k} \times \nabla q$ where q is a tracer conserved along a Lagrangian trajectory and \mathbf{k} is the vertical unit vector, as shown by P. Constantin, A. J. Majda, and E. Tabak, "Formation of strong fronts in the 2-D quasigeostrophic thermal active scalar," *Non-linearity* **7**, 1495 (1994).
- ¹⁶B. J. Cantwell, "Exact solution of a restricted Euler equation for the velocity gradient tensor," *Phys. Fluids A* **4**, 782 (1992).
- ¹⁷K. Ohkitani, "Some mathematical aspects of 2D vortex dynamics," in *Proceedings of Partial Differential Equations and Applications*, edited by D. Chae, Lecture Notes Series 38 (Seoul National University, 1995).
- ¹⁸K. K. Nomura and G. K. Post, "The structure and dynamics of vorticity and rate of strain in incompressible homogeneous turbulence," *J. Fluid Mech.* **377**, 65 (1998).
- ¹⁹E. Dresselhaus and M. Tabor, "The stretching and alignment of material elements in general flow fields," *J. Fluid Mech.* **236**, 415 (1991).
- ²⁰D. G. Dritschel, P. H. Haynes, M. N. Juckes, and T. G. Shepherd, "The stability of a two-dimensional vorticity filament under uniform strain," *J. Fluid Mech.* **230**, 647 (1991).
- ²¹D. G. Dritschel, "Vortex properties of two-dimensional turbulence," *Phys. Fluids A* **5**, 984 (1993).
- ²²Note that if $r = \cos 2\gamma$ then $\sqrt{(1-r)/(1+r)} = |\tan \gamma|$.
- ²³B. L. Hua, J. C. McWilliams, and P. Klein, "Lagrangian accelerations in geostrophic turbulence," *J. Fluid Mech.* **366**, 87 (1998).
- ²⁴P. Klein, B. L. Hua, and G. Lapeyre, "Alignment of tracer gradients in two-dimensional turbulence using second order Lagrangian dynamics" (in preparation for *Physica D*).